ISSN: 2633-4828 Vol. 5 No.2, June, 2023

International Journal of Applied Engineering & Technology

BEHAVIOR OF COLD-FORMED STEEL SINGLE AND COMPOUND ANGLES UNDER COMPRESSION

Samik Banerjee and Dr. Prashant S. Lanjewar
Department of Civil Engineering, Dr. A. P. J. Abdul Kalam University, Indore, MP, India
samik.banerjee90@gmail.com and pslanjewar@yahoo.com

ABSTRACT

This research investigates the behavior of cold-formed steel (CFS) single and compound angles under compression. The study explores the load-carrying capacity, deformation characteristics, and failure modes of these structural elements. A comprehensive experimental program was conducted, utilizing three distinct boundary conditions: pin-ended, fixed-ended, and partially restrained. Additionally, a series of numerical analyses were performed using ANSYS finite element software to validate and expand upon the experimental findings. The results demonstrate that lip stiffeners significantly enhance the load-carrying capacity of both single and compound angles. Specifically, lip stiffeners increased the load capacity by up to 20% for single angles and up to 40% for compound angles. The study also highlights the influence of different boundary conditions on the structural performance of cold-formed steel angles. The findings provide critical insights for the design and application of cold-formed steel structures in various engineering fields.

Keywords: Cold-formed steel, single angles, compound angles, compression behavior, load-carrying capacity, deformation characteristics, failure modes, boundary conditions, lip stiffeners, ANSYS finite element analysis.

1. INTRODUCTION

Cold-formed steel (CFS) has become increasingly popular in modern construction due to its high strength-to-weight ratio, ease of fabrication, and cost-effectiveness. Its versatility allows for the creation of various structural shapes, including single and compound angles, which are widely used in applications such as framing, bracing, and load-bearing components. Understanding the behavior of these structural elements under compression is essential for ensuring safety and optimizing design in engineering practices.

Cold-formed steel angles are typically manufactured by bending thin steel sheets at ambient temperatures, resulting in a lightweight yet strong material. These angles can be categorized into single angles (one bend forming an "L" shape) and compound angles (multiple bends forming more complex cross-sections). Each type exhibits distinct mechanical properties and performance characteristics when subjected to compressive loads.

Previous research has focused on the general behavior of cold-formed steel elements under various loading conditions. For instance, Murray and Sherief (1995) examined the American Institute of Steel Construction (AISC) design methodology for load and resistance factor design (LRFD) and the allowable stress design (ASD) methods, highlighting discrepancies in the treatment of local buckling and load distribution in steel members . Chou et al. (1996) evaluated the accuracy of existing design standards, including the American Iron and Steel Institute (AISI) and British Standards (BS: 5950), for cold-formed steel sections. Their findings underscored the variability in code predictions based on cross-sectional geometry and highlighted the need for more comprehensive guidelines .

Leach and Davies (1996) investigated the flexural behavior of thin-walled CFS beams, revealing significant impacts of local and distortional buckling on load-carrying capacity. Their research emphasized the necessity of incorporating these effects into design models to improve prediction accuracy . Pantelides (1996) extended this work by analyzing the influence of geometric imperfections and residual stresses on the stability of CFS columns, demonstrating that these factors could substantially reduce the ultimate strength of the members .

Cedric Marsh (1997) focused on the impact of corner radii in cold-formed steel sections, finding that smaller radii could lead to stress concentrations and reduced member capacity. This study suggested that optimizing corner

radii could enhance the performance of CFS angles under compression . Schafer and Pekoz (1998) contributed to the understanding of cold-formed steel behavior by developing advanced computational models to predict the performance of these members more accurately. Their work highlighted the importance of considering both local and global buckling modes in design .

Building on these foundational studies, this research aims to comprehensively investigate the behavior of cold-formed steel single and compound angles under compression. The study will assess the load-carrying capacity, deformation patterns, and failure modes of these elements through a combination of experimental testing and finite element analysis (FEA). The influence of boundary conditions and the presence of lip stiffeners will be evaluated to provide a detailed understanding of their effects on structural performance. The findings of this research will contribute to the development of improved design guidelines and standards for cold-formed steel structures, ultimately enhancing their safety and efficiency in engineering applications.

2. REVIEW OF LITERATURE

The study of cold-formed steel (CFS) structural elements, particularly under compressive loads, has been a subject of extensive research due to their widespread use in construction and engineering. This literature review synthesizes the findings of key studies to provide a comprehensive understanding of the behavior and design of CFS single and compound angles under compression.

Al-bermani and Kitipornchai (2003) conducted a numerical simulation to analyze the structural behavior of transmission towers, which provided insights into the stability and load-carrying capacities of thin-walled structures. Their study highlighted the importance of accurate modeling techniques in predicting the performance of CFS elements under various loading conditions .

The ASTM 370-92 (1996) standard outlines the test methods and definitions for mechanical testing of steel products. This standard is crucial for determining the mechanical properties of steel, which are essential for the design and analysis of CFS structures .

Bambach and Rasmussen (2004) explored design provisions for sections containing unstiffened elements with stress gradients. Their research in the Journal of Structural Engineering emphasized the need for specific design guidelines to account for the unique stress distribution in CFS sections, improving the reliability of structural designs .

Becque and Rasmussen (2008) investigated the interaction of local and overall buckling in stainless steel columns through numerical methods. Their findings provided a basis for developing design methods that can predict failure modes more accurately in CFS columns, emphasizing the need for considering both local and global buckling effects in design .

ABAQUS (2008) is a widely used finite element analysis (FEA) software that supports the modeling and analysis of complex structures, including CFS elements. The capabilities of ABAQUS have been instrumental in advancing the understanding of the mechanical behavior of CFS structures under various loading conditions .

The AISI S100-2007 (2007) and AISI Manual (1996) provide the North American specifications for the design of CFS structural members. These guidelines are fundamental for engineers and designers, offering detailed procedures for the design and analysis of CFS elements .

Anbarasu and Ashraf (2016) studied the behavior and design of cold-formed lean duplex stainless steel lipped channel columns, revealing the complexities involved in the distortional-global buckling mode interaction. Their experimental results contributed to a better understanding of the buckling behavior in thin-walled lipped channel sections.

Further research by Anbarasu and Murugapandian (2016) focused on the distortional-global buckling mode interaction in thin-walled lipped channels. This study provided valuable experimental data on the load-bearing capacity and failure modes of CFS elements.

Anbarasu et al. (2014a) examined the capacity of CFS built-up battened columns under axial compression, highlighting the structural performance of these columns and proposing new design considerations for improving their load-carrying capacities . Additionally, Anbarasu et al. (2014b) investigated the behavior and strength of CFS web-stiffened built-up battened columns, further enhancing the understanding of complex CFS column configurations.

AS/NZS 4600:2005 and the earlier AS/NZS 4600 (1996) standards provide guidelines for the design of CFS structures in Australia and New Zealand. These standards are crucial for ensuring the safety and reliability of CFS structures in these regions.

Bakker and Pekoz (2003) discussed the fundamental principles of the finite element method (FEM) for thin-walled members, emphasizing its application in analyzing CFS structures. Their work has been pivotal in advancing FEM techniques for evaluating the performance of thin-walled CFS elements .

Bebiano et al. (2008) developed GBTUL1.0b, a code for buckling and vibration analysis of thin-walled members, providing a powerful tool for engineers to analyze and design CFS structures. This code has been widely used in research and practice to predict the behavior of thin-walled members under various loading conditions . Finally, Becque (2008) in his PhD thesis, investigated the interaction of local and overall buckling in cold-formed stainless steel columns, contributing significantly to the theoretical understanding and practical design of CFS columns.

3. EXPERIMENTAL INVESTIGATION

3.1 Test Specimens

The examples are tried as combined box point segments as

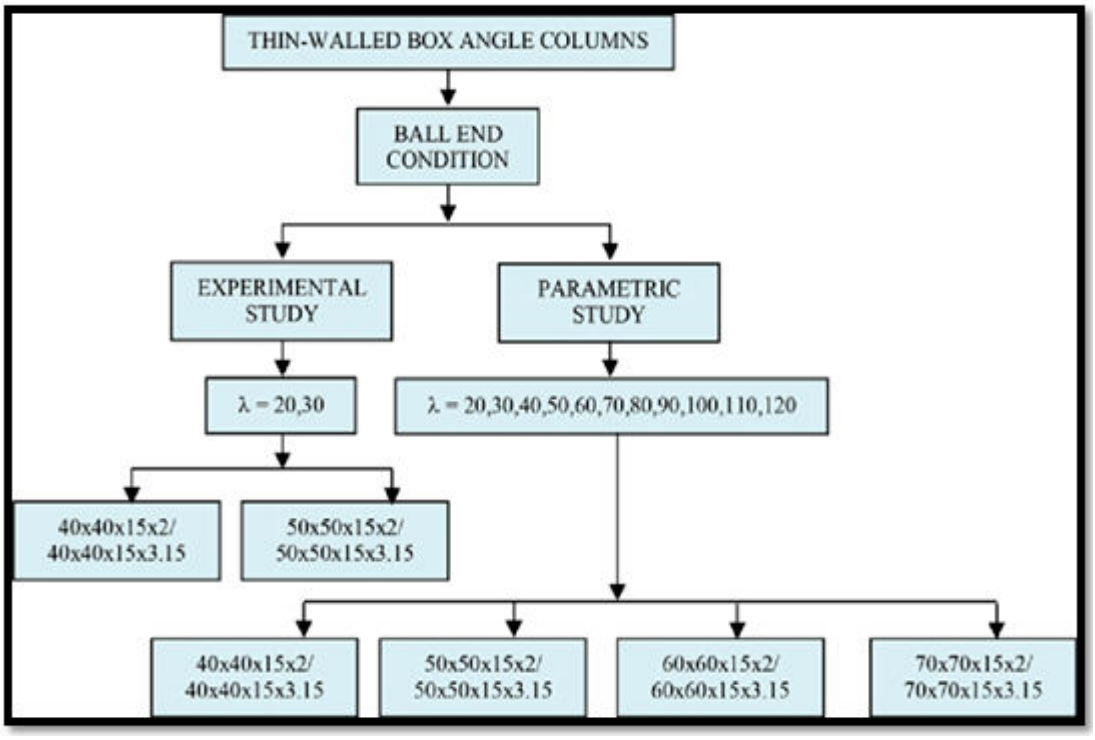

Figure: 1. Information about the study

Shown in Fig. 1 that can be connected in a reasonable way by using self-boring screws up to the limit set by NAS (2007) detail.

3.2 Material Properties

In this study, the examples were made using virus-framed steel sheets with thicknesses ranging from 2.0 to 3.15 mm. These steel sheets have many different properties. According to ASTM A 370 (1996), three strain tests are set up and analyzed so that the yield pressure, a definitive tractable pressure, and the percentile an incentive for the material are found. Because cold-framed steel gives way slowly, the offset method was used to figure out the yield pressure. Table 1 shows the average change from 0.2% balance of Young's modulus, yield stress, limit stress, and elongation. According to NAS rules, the strength of the final steel should be 289-584 N / mm2 and the ratio of tensile strength to yield strength should be 1.21-1.8. The NAS also states that the peak yield shouldbe 172 to 482 N / mm2. The lowest percentage of NAS stretches are believed to be between 12 and 27.

Figure 2 shows how the pressure coupons usually behave in terms of pressure and strain. The NAS Manual shows that the chosen steel's Yield Strength, Ultimate Tensile Strength, and Stretched Rate are all listed. It meant that each part should be strong, and sections fail because the area and the flexural clasping around the weaker tomahawks of the locations. The length of the stub sections was decided by what the Technical Memorandum in the Structural Stability Research Council guide said should be done. In the update, it was suggested that the length of the stub segment shouldn't be less than multiple times the best areas' aspect and shouldn't be bigger than multiple times the Radius of Gyration about the segment's powerless pivot. This is based on BS 5950-Part-5 (1987)

Table: 1 Coupon: How They Are Made

Type Of Steel	Thickness (mm)	Modulus of Elasticity Mpa	Yield Stress(fy)MPa	Ultimate Stress (fu) Mpa	fu/fy	% Elongation
1	3.01	1585215	582	582	2.25	20
2	3.5	3125282	325	845	3.12	15

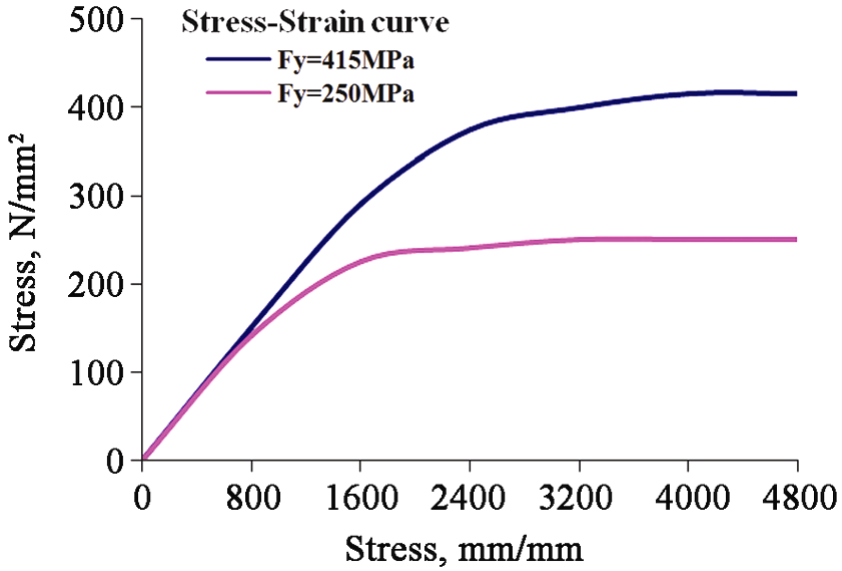

Figure: 2 Stress-Strain Behaviors of Tensile Coupons

3.3 Test Details

In the Universal Testing Machine, the tests are done. Only sixteen short and stub sections of the right size and shape are cut to the right length and to a thickness of 6 mm. 120 x 120 mm plates are welded to the ends of the examples so that the middle of the plate is in the same place as the centroid of the examples. This allows the pivotal load to be used through the centre of gravity. To use weight pivotally, you need two plates that are 12 mm thick and 120 mm by 120 mm, with a round hole in the middle so that a ball with a 40 mm diameter can fit

between them. These plates are connected to the focuses of the first two plates. The end base plate and the example closes are both made by a machine so that the jack can sit in the best place. The verticality of the example is checked with plumb weave and soul level in two different directions. The examples are stacked up so that the middle of the developed segment is in the middle of the stack. Dial checks with a count of 0.01 or less are kept so that the vertical and flat avoidance can be measured. To keep track of how much the hubs of the test samples shrunk, a dial measure was set up so that its end would touch the moving top of the segment testing machine. When the example was in the flexible range, axial load grew quickly. When the example was in the plastic range, axial load grew much more slowly until the example fell apart. Figure 5 shows a diagram of how the test set up works in the Universal Testing Machine.

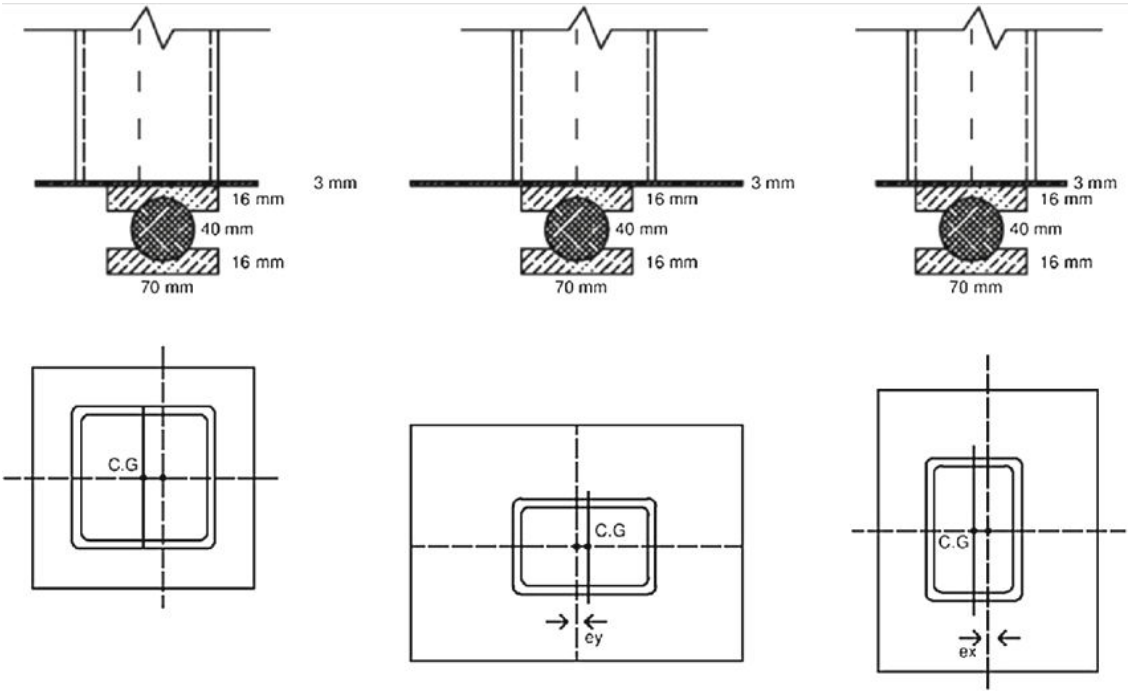

Figure: 3 Ball End Condition

3.4 Compression Test

Set up Compression tests were completed on a segment testing machine. The test examples were associated with the end apparatuses and were tried to disappointment. In each test, the load on the hub increased slightly faster in the flexible range and slightly slower in the plastic range, until the example fell. Mitutoyo and Batty dial checks of least count 0.01 mm were utilized to quantify the pivotal shortening and parallel avoidances of the part. Dial checks were put in the middle of the part and one-fourth of the way up the level of the area. The tips of the dial checks touched the web and rib of the examples to measure the parallel redirections. One dial check was placed so that its tip touched the portable top of the segment testing machine. This was done to measure how much the test example had shrunk at its pivot point. Electrical resistance strain checks of type BKSA 20 with a check component of 2.1 0.6 were used to measure the endure mid-level. The spines in the middle of the example were fitted with strain gauges. Care was taken that these strain measures were fixed farther away from the nonpartisan pivot and to check whether the cross-segments experience symmetric or unsymmetrical clasping. Strain marker with 10 channels was utilized to record the strain estimations. The strain measure and dial check readings were taken at higher stretches in the versatile reach and at closer spans in the inelastic reach until the example fizzled. Figure 4 shows the test set up for darted end association

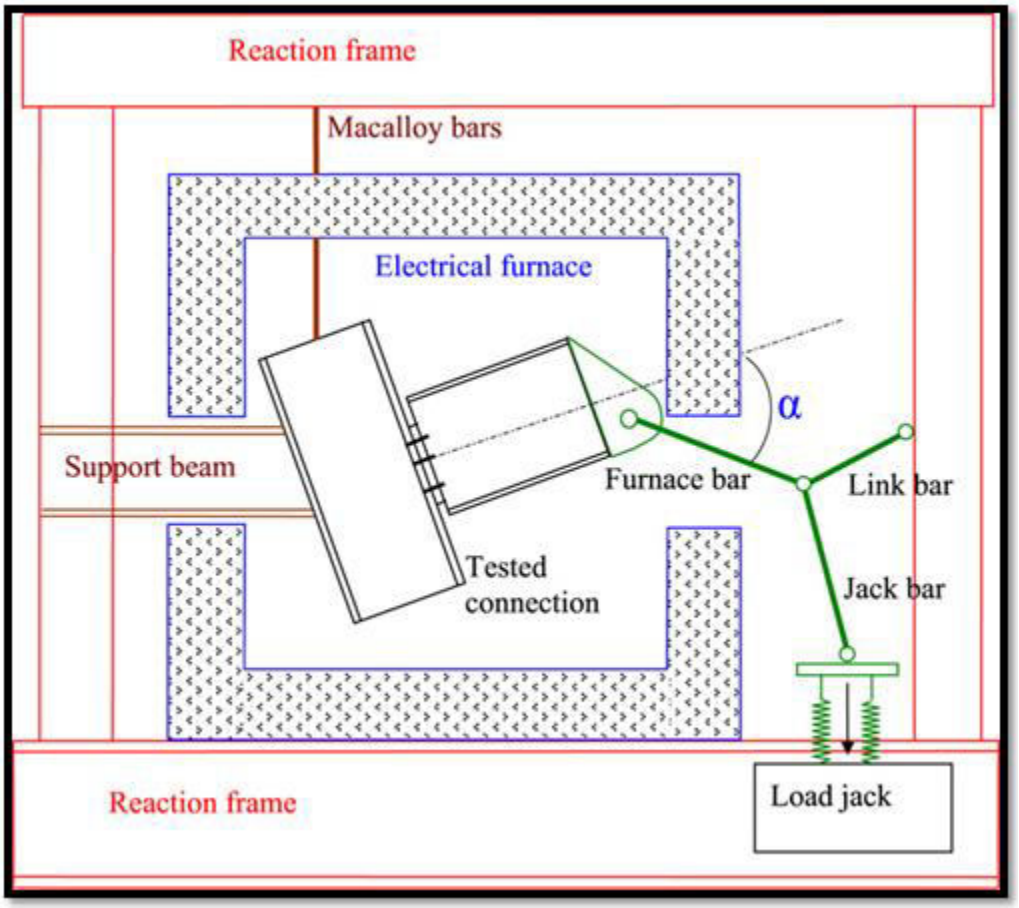

Figure: 4 TestSet Up for Bolted End Connection

4. Finite Element Modeling

4.1 General

Here, the Finite Element Program using ABAQUS (2010) was used to make a mathematical model of the two-point segments that had been made. The non-linear FEA was done with ABAQUS to predict the main idea of cold-shaped areas that formed under hub stacking. During the Finite Element Analysis (FEA), the real cross-sectional and material properties of the examples were used, and the models were drawn based on the real cross-sectional properties of the middle line. A simple model with a reasonable calculation time and level of complexity was made to figure out what the final limit is and how the developed people deal with disappointment. The most important thing was to find the right balance between accuracy and skill. Because there isn't enough information about the profile, the remaining weight on a final load and the starting plastic strains from snaking and corner cold-bowing aren't taken into account as Schafer and Pekoz did (1998)

4.2 Element Type,

Size of the Network and Material Model Modeling of examples is done with the help of a four-noded S4R5 light shell component with six levels of freedom for each hub, which is based on the ABAQUS model. A union test was done on the segment to find a Finite Element network that would work for dissecting. In the leg and lip parts, the component viewpoint proportion (length to width) was set around 1.0 to get very accurate results with a lot less computing time. For the different segments, the 10 10 mm2 component network sizes were used. As shown in Fig. 6, the regular designs for a Finite Element network and the clasping mode with the limit standards for confine point areas are shown.

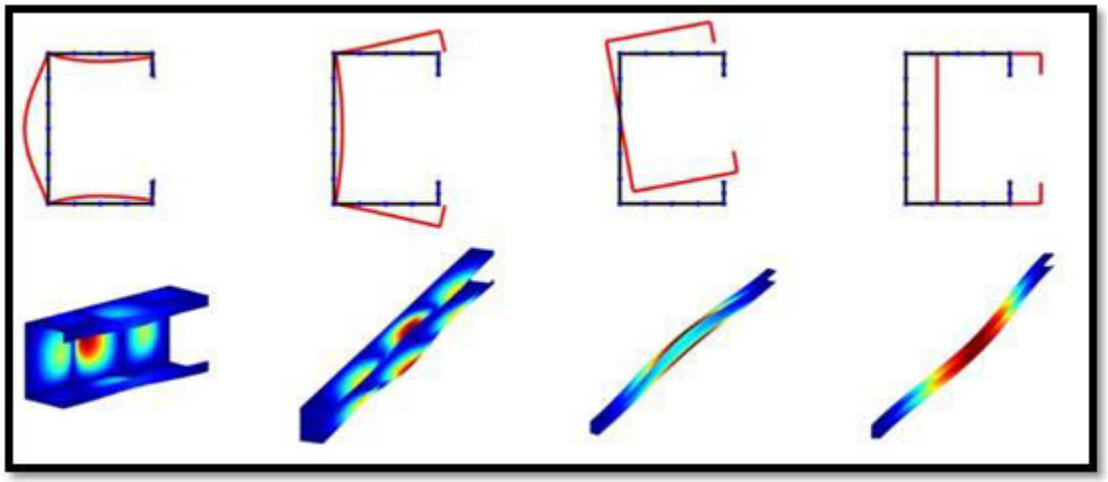

Figure: 6A typical finite element meshes with local and deformational modes of buckling

5. RESULT AND DISCUSSION

The behavior of thin-walled steel box angle sections under axial compression was investigated. Axial shortening behavior and lateral deflection behavior concerning load were extensively studied across various stages of loading.

The study considered how cold-formed steel single angles, double angles welded together, and compound angles would behave under axial compression. The research examined the relationship between load and axial shortening, load and lateral deflection, and load and strain under both elastic and plastic loading conditions. Factors such as slenderness ratio, cross-sectional geometry of the angle, type of steel, and the width-to-thickness ratio of the angle were analyzed for their impact on load-carrying capacity. Additionally, the effects of symmetry and buckling mode of the angles were also explored.

5.1 Experimental Results

The examination results from the trials were validated by comparing the outcomes of Finite Element Analysis (FEA) and the Direct Strength Method (DSM). The test samples, assembled with 6 mm self-drilling screws, were included in the FEA simulations. Additionally, end segment cross-sectional distortion was minimized by using thick end plates that replicated the end conditions during the experimental setup.

Table 2 presents the comparison of the experimental ultimate loads (Ptest) with the ultimate loads (PFEA) determined via FEA and DSM. The average and standard deviation of the ratio of FEA to experimental ultimate load-carrying capacity were 1.02 and 0.05, respectively. Similarly, the average and standard deviation of the ratio of FEA to DSM ultimate load-carrying capacity were 1.01 and 0.05, respectively. Overall, the ultimate loads and the failure mode patterns predicted using FEA closely matched the experimental ultimate loads for all sections.

5.2 Carrying a Load

Limit Table 2 shows how the DSM expects the unfactored plan strength to turn out. For areas with a thickness of 2 mm, the FEA results are higher than the exploratory results by up to 16%, except for LAB-50-50-15-2-20, which was off by 2%. Aside from a few examples, FEA's estimates of the strength of the expected heavy loads are off by up to 6 percent. FEA showed that the expected range for samples with a thickness of 3.15 mm had grown by 3 percent, while the DSM showed that the request rate had gone down by 13 percent. No matter how thick the examples were, every one of the 16 examples bombed.

Table 2: Compression between EFA and DSA results from experiments for Box Section

s.no	Speciemen	λ	Length	Screw Spacing	FEA	Exp	DSM	FEA/EXP	FEA/DSM
2mm Thickness									
1	**40×50×14**	**50**	**402.11**	**152.1**	**110.44**	**200.6**	**250**	**2.29**	**2.00**
2	50× 30 × 11	60	503.55	173.5	115.88	105.6	150.63	3.58	1.22
3.15 mm Thickness									
1	**30× 20 × 2**	**40**	**503.12**	**172.2**	**201.5**	**551.63**	**300.8**	**400**	**4.01**
2	40×10×4	60	601.55	191.5	181.5	612.71	350.9	180.96	3.11
Mean									
Standard Division									

6. CONCLUSION

Based on the compression tests conducted on single angles, double angles welded back-to-back, and lipped angles, the following conclusions can be drawn:

- For angles tested with welded end connections, increasing the slenderness ratio from 15 to 30 decreases the ultimate load-carrying capacity by 15% for single angles and 10% for double and lipped angles.
- The ultimate loads of double and lipped angles with welded end connections are 2.10 and 2.20 times greater, respectively, than those of single angles when tested as stub columns.
- For specimens with a higher width-to-thickness ratio, non-linearity in axial shortening behavior begins at 40% of the ultimate load, whereas for smaller width-to-thickness ratios, non-linearity begins at 50%. The behavior is more pronounced for stub columns compared to short columns.
- The initial stiffness of lipped angles is twice that of single angles and one and a half times that of double angles when tested as stub columns with welded end connections.
- The ductility coefficient of angles with welded ends is 50% higher compared to angles with pinned ends. Additionally, the ductility coefficient of angles with bolted ends is twice that of angles with pinned ends.
- For double angles with welded ends, the compressive stress at the toe end of the free legs converts to tensile stress at 75% of the ultimate load.
- Double angles welded back-to-back with bolted ends failed by local buckling occurring at the end of the column or at one-fourth the height, while lipped angles with welded ends also failed by local plate buckling at mid-height.
- Single angles tested as short columns with bolted ends failed by flexural buckling at one-fourth the height, whereas lipped angles tested as short columns with bolted ends failed by torsional buckling

REFERENCES

1. Al-bermani F.G.A. and Kitipornchai S. (2003), 'Numerical Simulation of Structural Behaviour of Transmission Towers', Thin-Walled Structures, Vol. 41, No. 2-3, pp. 167-177.
2. ASTM : 370 - 92 (1996), 'Standard Test Methods and Definitions for Mechanical Testing of Steel Products.
3. Bambach M.R. and Rasmussen K.J.R. (2004), 'Design Provisions for Sections Containing Unstiffened Elements with Stress Gradient', Journal of Structural Engineering, ASCE, Vol. 130, No. 10, pp. 1620-1628.

4. Becque J and Rasmussen KJR (2008) Numerical investigation and design methods for stainless steel columns failing by interaction of local and overall buckling. Research Report, No. 888. Sydney, NSW, Australia: School of Civil Engineering, University of Sydney

5. ABAQUS (2008) ABAQUS Standard (Version 6.12). Johnston, RI: Simulia Inc. AISI S100-2007 (2007) North American specification for the design of cold-formed steel structural members.

6. AISI Manual (1996), 'Cold-formed Steel Design Manual', American Iron and Steel Institute.

7. AISI S100-2016 (2016) North American specification for the design of cold-formed steel structural elements. Anbarasu M and Ashraf M (2016) Behaviour and design of cold-formed lean duplex stainless steel lipped channel columns. Thin-Walled Structures 104: 106–115.

8. Anbarasu M and Murugapandian G (2016) Experimental study on distortional-global buckling mode interaction on the thin-walled lipped channel. Materials and Structures 49(4): 1433–1442.

9. Anbarasu M, Bharath Kumar P and Sukumar S (2014a) Study on the capacity of cold-formed steel built-up battened columns under axial compression. Latin American Journal of Solids and Structures 11(12): 2271–2283.

10. Anbarasu M, Kanagarasu K and Sukumar S (2014b) Investigation on behaviour and strength of cold-formed steel web-stiffened built-up battened columns. Materials and Structures 48(12): 4029–4038. AS/NZS 4600:2005 (2005) Cold-formed steel structures.

11. AS/NZS : 4600 (1996), 'Cold-formed Steel Structures', Australia/New Zealand Standard.

12. Bakker M.C.M. and Pekoz T. (2003), 'The Finite Element Method for Thin-walled Members - Basic Principles', Thin-Walled Structures, Vol. 41, No. 2-3, pp. 179-189.

13. Bebiano R, Silvestre N and Camotim D (2008) GBTUL1.0b – code for buckling and vibration analysis of thin-walled members. Available at: http://www.civil.ist.utl.pt/gbt Becque J (2008) The interaction of local and overall buckling of cold-formed stainless steel columns. PhD Thesis, University of Sydney, Australia

14. Ben Young (2004), 'Tests and Design of Fixed-Ended Cold-Formed Steel Plain Angle Columns', Journal of Structural Engineering, ASCE, Vol. 130, No. 12, pp. 1931-1940.

15. Ben Young (2005), 'Experimental Investigation of Cold-formed Steel Lipped Angle Concentrically Loaded Compression Members', Journal of Structural Engineering, ASCE, Vol. 131, No. 9, pp. 1390-1396.

16. Ben Young and Ehab Ellobody (2005), 'Buckling Analysis of Coldformed Steel Lipped Angle Columns', Journal of Structural Engineering, ASCE, Vol. 131, No. 10, pp. 1570-1579.

17. Ben Young and Rasmussen K.J.R. (1999), 'Behaviour of Cold-formed Singly Symmetric Columns', Thin-Walled Structures, Vol. 33, No. 2, pp. 83-102.

18. Dabaon M, Ellobody E and Ramzy K (2015) Experimental investigation of built-up cold-formed steel section battened columns. Thin-Walled Structures 92: 137–145.

19. El Aghoury MA, Salem AH, Hanna MT, et al. (2013) Ultimate capacity of battened columns composed of four equal slender angles. Thin-Walled Structures 63: 175–185.

20. Fratamico DC, Torabian S, Rasmussen KJR, et al. (2016) Experimental investigation of the effect of screw fastener spacing on the local and distortional buckling behavior of built-up cold-formed steel columns. In: Proceedings of the Wei-Wen Yu international specialty conference on cold formed steel structure, Baltimore, MD, 9–10 November

21. Murray, T. M., & Sherief, M. A. (1995). Analysis of load and resistance factor design for cold-formed steel structures. Journal of Structural Engineering, ASCE.

22. Chou, C. C., Chen, W. F., & Yu, W. W. (1996). Assessment of cold-formed steel design standards. Journal of Constructional Steel Research.

23. Leach, P., & Davies, J. M. (1996). Flexural behavior of thin-walled cold-formed steel beams. Thin-Walled Structures.

24. Pantelides, C. P. (1996). Stability of cold-formed steel columns with geometric imperfections. Journal of Structural Engineering, ASCE.

25. Marsh, C. (1997). Influence of corner radii on the strength of cold-formed steel sections. Thin-Walled Structures.

26. Schafer, B. W., & Pekoz, T. (1998). Computational modeling of cold-formed steel behavior. Journal of Structural Engineering, ASCE.